Heliyon 6 (2020) e03261

Contents lists available at ScienceDirect

Heliyon

journal homepage: www.cell.com/heliyon

Research article

A human somatic cell culture system for modelling gene silencing by transcriptional interference

Theresa Kühnel [a], Helena Sophie Barbara Heinz [a], Nadja Utz [a,b], Tanja Božić [c], Bernhard Horsthemke [a], Laura Steenpass [a,*]

[a] Institute of Human Genetics, University Hospital Essen, University Duisburg-Essen, Hufelandstr 55, 45147 Essen, Germany
[b] Present address: Institute of Neuropathology, Justus Liebig University Giessen, Aulweg 128, 35392 Giessen, Germany
[c] Helmholtz Institute for Biomedical Engineering, Division of Stem Cell Biology and Cellular Engineering, RWTH Aachen University Medical School, Pauwelsstr. 20, 52074 Aachen, Germany

ARTICLE INFO

Keywords:
Genetics
Molecular biology
Epigenetics
Gene expression
Gene regulation
Human genetics
Genetic disorders
Gene expression
Genomic imprinting
Methylation
Transcriptional read-through.

ABSTRACT

Transcriptional interference and transcription through regulatory elements (transcriptional read-through) are implicated in gene silencing and the establishment of DNA methylation. Transcriptional read-through is needed to seed DNA methylation at imprinted genes in the germ line and can lead to aberrant gene silencing by DNA methylation in human disease. To enable the study of parameters and factors influencing transcriptional interference and transcriptional read-through at human promoters, we established a somatic cell culture system. At two promoters of imprinted genes (*UBE3A* and *SNRPN*) and two promoters shown to be silenced by aberrant transcriptional read-through in human disease (*MSH2* and *HBA2*) we tested, if transcriptional read-through is sufficient for gene repression and the acquisition of DNA methylation. Induction of transcriptional read-through from the doxycycline-inducible CMV promoter resulted in consistent repression of all downstream promoters, independent of promoter type and orientation. Repression was dependent on ongoing transcription, since withdrawal of induction resulted in reactivation. DNA methylation was not acquired at any of the promoters. Overexpression of DNMT3A and DNMT3L, factors needed for DNA methylation establishment in oocytes, was still not sufficient for the induction of DNA methylation. This indicates that induction of DNA methylation has more complex requirements than transcriptional read-through and the presence of de novo DNA methyltransferases.

1. Introduction

Genomic imprinting is an epigenetic process resulting in monoallelic parent-of-origin dependent gene expression, regulated by differential DNA methylation (Horsthemke, 2014). DNA methylation is established in only one of the parental germ lines on specific regulatory regions, called gametic differentially methylated regions (gDMRs). Methylation analysis of gDMRs in somatic cells typically shows ~50 percent methylation, as one parental allele is fully methylated whereas the other one is unmethylated. This differential DNA methylation is stable throughout development and cellular differentiation. The process of transcription plays an essential role in the establishment of DNA methylation at gDMRs and in the regulation of imprinted gene expression by transcriptional interference. Both levels of regulation by transcription have been observed at the Prader-Willi syndrome (PWS)/Angelman syndrome (AS) imprinted gene cluster on human chromosome 15 (Figure 1A). The gDMR resides in a CpG island at the *SNURF-SNRPN* promoter/exon 1, which becomes methylated in the female germ line only (Horsthemke, 2014). Maternal-only methylation of the PWS-SRO is seen after next generation bisulfite sequencing of DNA extracted from peripheral blood cells, with ~50% of the reads representing the methylated maternal allele and ~50% of reads representing the non-methylated paternal allele (Figure 1B). In humans, the gDMR is part of a bipartite imprinting center, which consists of the AS-SRO (Angelman syndrome - shortest region of overlap) and the PWS-SRO (Prader-Willi syndrome – shortest region of overlap), the latter of which is identical with the gDMR at the *SNURF-SNRPN* promoter (Buiting et al., 1999). The upstream AS-SRO serves as oocyte-specific promoter initiating transcriptional read-through resulting in establishment of DNA methylation at the PWS-SRO (Figure 1C, Lewis et al., 2015; Lewis et al., 2019). Transcription from *Snrpn* upstream promoters is also essential for imprint establishment in the mouse (Smith et al., 2011). DNA methylation of the

* Corresponding author.
E-mail address: laura.steenpass@uni-due.de (L. Steenpass).

https://doi.org/10.1016/j.heliyon.2020.e03261
Received 6 December 2019; Received in revised form 6 January 2020; Accepted 15 January 2020

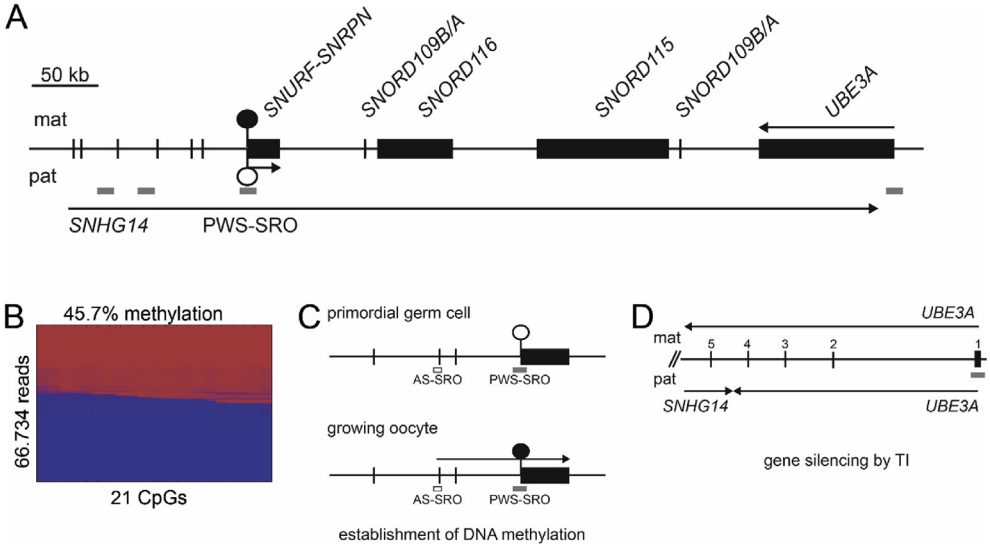

Figure 1. Imprint establishment and silencing of paternal *UBE3A* by transcription. A) Schematic view of PWS/AS locus on human chromosome 15. Imprinted expression in neurons is shown on the maternal (mat) and paternal (pat) chromosome. Vertical bars and boxes: exons, arrows: active transcription and direction, grey horizontal lines: CpG islands, lollipop: filled: methylated, white: not methylated, SRO: shortest region of overlap. B) Heatmap as output of quantitative methylation analysis by next-generation bisulfite sequencing. PWS-SRO was analyzed in blood of a normal control person. 66.734 total reads are depicted in rows, 21 CpG sites in columns. Methylated CpGs appear in red, non-methylated CpGs in blue. Fully methylated reads (red) at the top are derived from the maternal allele, non-methylted reads (blue) at the bottom from the paternal allele, resulting in 45.7% overall methylation. C) Imprint establishment at PWS-SRO by transcriptional read-through initiating at AS-SRO in growing oocytes (bottom), but not in primordial germ cells (top). D) Silencing of paternal *UBE3A* by RNA polymerase II collision between *SNHG14* and *UBE3A* transcripts in intron 4.

PWS-SRO on the maternal chromosome represses transcription of *MRKN3*, *MAGEL2*, *NDN*, *SNRPN* and *SNHG14,* which serves as a host gene for snoRNAs. These genes are only active and transcribed from the paternal chromosome (Figure 1A, Horsthemke, 2014). In neurons, *SNHG14* transcription overlaps the *UBE3A* gene, which is transcribed from the opposite strand (Hsiao et al., 2019; Landers et al., 2004; Rougeulle et al., 1998). As shown in the mouse, the convergent promoter arrangement of *Snhg14*and *Ube3a* leads to silencing of the paternal *Ube3a* allele as a result of RNA polymerase collision (Figure 1D; Meng et al., 2013; Numata et al., 2011). However, the *Ube3a* promoter does not become methylated upon silencing (Meng et al., 2013). Similar to silencing of paternal *Ube3a* by *Snhg14*, predominant maternal expression of *Commd1* at the murine imprinted *Commd1/Zrsr1* locus is caused by sense – antisense transcriptional interference and transcriptional suppression of *Commd1* on the paternal allele (Joh et al., 2018). At the human *RB1* locus, transcription is biased towards the maternal allele, which is likely to be regulated by transcriptional interference between regular *RB1* and the alternative transcript *RB1-E2B* starting in intron 2 of *RB1* (Kanber et al., 2009). Transcriptional interference and transcriptional read-through can occur together, as has been demonstrated at the murine imprinted *Igf2r/Airn* locus. Here, stable repression of the paternal *Igf2r* promoter by DNA methylation is dependent on traversing transcription of *Airn* (Latos et al., 2009, 2012).

The necessity of transcription through the gDMR for establishment of DNA methylation has further been demonstrated at the imprinted *Kcnq1*, *Gnas* and *Zrsr1* loci in mouse oocytes (Chotalia et al., 2009; Joh et al., 2018; Singh et al., 2017). Patients carrying mutations that abolish activity of the *KCNQ1* promoter on their maternally inherited chromosome 11 lack DNA methylation at the gDMR *KCNQ1OT1:TSS-DMR* imprinting center and develop the imprinting disorder Beckwith-Wiedemann syndrome (Beygo et al., 2019; Valente et al., 2019). This suggests the need for *KCNQ1* transcription through the gDMR for establishment of DNA methylation in human oocytes. DNA methylation at gDMRs in the oocyte is likely to be established by the same mechanism as gene-body methylation during active transcription (Kelsey and Feil, 2013; Veselovska et al., 2015). Actively transcribed genes or regions are marked by the histone modification H3K36me3 (trimethylation of lysine 36 of histone H3), which results in recruitment of de novo DNA methyltransferases and the deposition of DNA methylation in gene bodies (Baubec et al., 2015; Dhayalan et al., 2010). In general, factors needed for DNA methylation mediated by transcription are therefore present in germ cells and somatic cells. However, Joh et al. demonstrated that de novo DNA methylation of the *Zrsr1*-DMR did only occur in the growing mouse oocyte but not during post-fertilization development (Joh et al., 2018). This points to oocyte-specific factors needed for imprint establishment.

Transcriptional interference is defined as the negative influence of one transcriptional process onto another in cis (Shearwin et al., 2005). Pervasive transcription of the human genome and the assumption that about 40% of all transcripts arise from overlapping genomic sequences has introduced transcriptional interference as an important regulatory process (Berretta and Morillon, 2009). Transcriptional interference arises at tandem and convergent promoters and involves different mechanisms, eg. promoter occlusion, roadblocking and RNA polymerase collision (Shearwin et al., 2005). The causal association of transcription traversing active promoters with induction of DNA methylation was supported further by genomic deletions of transcription termination signals found in patients. In Lynch syndrome, which is hereditary non-polyposis colorectal cancer (HNPCC), deletions of the termination signal of the upstream gene *EPCAM* resulted in transcriptional read-through of *EPCAM* across the *MSH2* promoter in sense direction and induction of DNA methylation (Figure S1A; Ligtenberg et al., 2009). In α-thalassemia a genomic deletion including the genes *HBA1*, *HBQ1* and the 3′-end of the downstream gene *LUC7L* resulted in an elongated *LUC7L* transcript that overlapped the *HBA2* gene in antisense direction. This led to DNA methylation and stable silencing of *HBA2* (Figure S1B; Tufarelli et al., 2003). In rare cases of the vitamin B12 metabolism cblC disorder, which is caused by defects in *MMACHC* gene expression, a splice site mutation in the neighbouring *PRDX1* gene leads to skipping of its last exon including the poly(A) signal and continuous transcription in antisense across the *MMACHC* gene and its promoter (Gueant et al., 2018). This resulted in DNA methylation and silencing of *MMACHC* expression on the allele carrying the mutation in *PRDX1*. This demonstrates that genetic lesions in neighboring genes, which lead to aberrant transcription elongation across gene promoters, can induce DNA methylation.

These findings resulted in our hypothesis that somatic cells harbor all necessary factors for de novo DNA methylation by transcriptional read-through. Transcriptional read-through at an active promoter will result

in transcriptional interference and might lead to DNA methylation. How these processes are linked, and which factors are needed or make promoters susceptible to the regulation by transcriptional read-through and transcriptional interference is not entirely clear. Current systems investigating transcriptional interference often employ yeast, bacteria or synthetic systems (Bordoy et al., 2016; Hobson et al., 2012; Saeki and Svejstrup, 2009). Although these systems allow straight forward generation of constructs and the use of reporter systems for read-out, they are not suited to study the complex epigenetic mechanisms occurring as a consequence of transcriptional read-through and interference in mammalian cells. DNA methylation at CpG sites is absent in yeast and bacteria (Capuano et al., 2014; Marinus and Løbner-Olesen, 2009). Moreover, in transient transfection systems, plasmid-based constructs do not integrate into the genome and are not influenced by large-scale chromatin interactions. A recent study employed mouse embryonic stem cells to study acquisition of DNA methylation at intragenic promoters by transcription (Jeziorska et al., 2017). The authors showed that methylation of intragenic CpG island promoters is related to traversing transcription, the presence of the histone modification H3K36me3 and relative promoter strength. Especially, induction of methylation was related to differentiation, mainly because transcription of the main promoter increased (Jeziorska et al., 2017). This study also supports the notion that germ line passage is not needed for transcription mediated establishment of DNA methylation.

Here we describe the generation of a simple and versatile human cell culture system to study transcriptional interference, transcriptional read-through and de novo DNA methylation. In this system, any promoter of interest (test promoter) can be cloned downstream of the inducible CMV promoter and the construct is inserted at one and the same genomic locus in the host cells, thus allowing comparisons between different experiments. Here, we tested the promoters of the non-imprinted *HBA2* and *MSH2* genes and the imprinted *SNRPN* and *UBE3A* genes.

2. Materials and methods

2.1. Generation of constructs

In brief, selected promoter fragments were amplified from genomic DNA of Flp-In T-REx 293 cells (Thermo Fisher Scientific, #78007; *UBE3A*, *MSH2* and *SNRPN*) or from plasmid pZErO-*HBA*4kb*Xho*I (*HBA2*) and verified by sequencing. Inserted and endogenous promoter sequences can be discriminated by single nucleotide variants. Promoter fragments were inserted into the pGL4.10 luciferase reporter vector (Promega, #E6651) and tested for promoter activity. The targeting vector for Flp-In T-REx cells, pcDNA5/FRT/TO (Thermo Fisher Scientific, #V6520-20), was modified and contains the rabbit β-globin (*ocHBB2*) partial exon 2–intron 2–exon 3 array, in which a cloning linker or an EcoRV restriction site was inserted in intron 2. The cloning linker and the EcoRV restriction site were used to integrate the minigenes that consist of a promoter fragment driving *EGFP* expression and promoter sequences containing exon 1 of the gene of interest ($MSH2^S$_ex1, $SNRPN^S$_ex1), respectively. To enlarge the distance between CMV and test promoters, constructs for $SNRPN^S$_GFP, $SNRPN^S$_ex1 and $MSH2^S$_ex1 contain a spacer sequence upstream of *ocHBB2* exon 2. Primers are listed in Table S1 and plasmids generated and used in this study are listed in Table S2. A detailed description of the cloning procedure is given in Supplementary Methods.

2.2. Generation and induction of stable cell lines

Flp-In T-REx 293 and Flp-In T-REx HeLa cells (Thermo Fisher Scientific) were maintained in Flp-In medium (DMEM,10% FBS, 1% penicillin/streptomycin (all Thermo Fisher Scientific, #41966, #10270, #15140122), 15 μg/ml blasticidin (Invivogen, #ant-bl-1)) containing zeocin (50 μg/ml for Flp-In T-REx 293 and 200 μg/ml for Flp-In T-REx HeLa; Invivogen, #ant-zn-1). For transfection, 1.5×10^5 cells/well were seeded in a 6-well plate (medium without antibiotics) and transfected using Lipofectamine 2000 reagent (Flp-In T-REx 293; Thermo Fisher Scientific, #11668019) or Fugene HD (Flp-In T-REx HeLa; Promega, #E2311) with 100 ng of minigene-BV-plasmids and 900 ng of plasmid pCSFLPe (Table S2). 24 hours after transfection cells were transferred to four 10 cm cell culture dishes. After another 24 h medium was changed to Flp-In medium with hygromycin (100 μg/ml for Flp-In T-REx 293, 250 μg/ml for Flp-In T-REx HeLa; Invivogen, #ant-hg-1). After 10 to 14 days of selection, single colonies were isolated and expanded. Success of minigene integration was monitored by *LacZ* staining of fixed cells (1% formaldehyde, 0.2% glutaraldehyde in PBS) stained with 5 mM $K_3[Fe(CN)_6]$, 5 mM $K_4[Fe(CN)_6]$, 2 mM $MgCl_2$, 1 mg/ml X-Gal in PBS for 2.5 h at 37 °C. Non-recombined cells stain blue, recombined cells do not. Three independent clonal cell lines per construct were used for further experiments. Induction of the CMV promoter was achieved by adding doxycycline to the medium (Sigma, #D9891, final concentration 1 μg/ml). Under induction, including non-induced control cells, medium was prepared using tetracycline-free FBS (Thermo Fisher, # 16000-044) and changed daily.

2.3. Isolation of DNA, RNA and protein

Isolation of DNA, RNA and protein was performed on 2×10^6 Flp-In T-REx 293 cells either simultaneously using the AllPrep DNA/RNA/Protein Mini Kit (Qiagen, #80004) or separately using RNeasy Mini Kit (Qiagen, #74104) and FlexiGene DNA Kit (Qiagen, #51206) according to manufacturer's instructions. Protein lysates were prepared in lysis buffer (500mM NaCl, 20mM Tris pH8.8, 1mM EDTA, 0.5% NP40, 1x Halt proteinase and phosphatase inhibitor (Thermo Fischer, #78442)). Samples were incubated on ice for 30 min with vortexing every 10 min. After centrifugation at 14.000 rpm for 20 min by 4 °C, the supernatant was aliquoted and frozen at -80 °C.

2.4. Quantitative RT-PCR

Total RNA was treated with RQ1 RNase-Free DNase (Promega, #M6101) and reverse transcribed into cDNA using the GeneAmp RNA PCR core kit and oligo-dT primers (Thermo Fisher Scientific, #N8080143). Quantitative real-time PCR was performed on a Roche LightCycler II using LightCycler 480 Probes Master Mix (Roche, #04887301001), probes from Roche universal probe library (UPL) and corresponding primers at following conditions: 95 °C, 10 min; 45 cycles 95 °C, 10 s, 60 °C, 30 s, 72 °C, 1 s; 40 °C, 30 s. Triplicate measurements were normalized to mean expression of *GAPDH* and calibrated to indicated samples. Primers and probes are listed in Table S1.

2.5. Western blot

Proteins were resolved on 10% SDS polyacrylamide gels and transferred to nitrocellulose membrane (Thermo Fisher Scientific, #GE10600016) by semi dry transfer. Membranes were blocked in 5% milk powder (Roth, #T145-2) or 5% Bovine Serum Albumin (BSA, Roth #8076.2) and incubated over night at 4 °C with primary antibodies (GFP: CST, #2956, 1:1000; GAPDH: CST, #2118, 1:5000, DNMT3A: Origene, #TA336580, 1:100; DNMT3L: Novus Biologicals, #H00029947-D01P, 1:500; -tubulin: CST, #2146S,1:1000). Detection was performed using HRP-conjugated secondary antibodies (Thermo Fisher Scientific, goat anti-rabbit #32460 and goat anti mouse #32430), Super Signal West Dura Extended Duration Substrate (Thermo Fisher Scientific, #34075) and development on X-ray film or INTAS Chemostar Touch 21.5 (1×1 binning or 4×4 binning, sequence images every 30sec). Images of complete membranes are displayed in Figures S11 - S13.

2.6. Analysis of DNA methylation

500 ng of genomic DNA was converted using the EZ DNA Methylation-Gold kit (Zymo Research, #D5006) according to

manufacturer's instructions. For the following PCR reaction, 1 µl of the bisulfite-converted DNA was mixed with 0.4 µM tagged, amplicon-specific primers and HotStarTaq Master Mix (Qiagen, #203443) in a total volume of 25 µl. PCR conditions were 95 °C for 15 min, (95 °C for 30 s, annealing temperature for 30 s, 72 °C for 45 s) 45 cycles, 72 °C for 10 min. For analysis by Sanger sequencing, PCR products were sequenced using tag-specific primers on an ABI 3130XL Genetic Analyzer. Sequencing analysis was performed using Geneious R10 (Biomatters). In the alignment, methylated cytosine residues appeared as cytosine, whereas non-methylated cytosine residues appeared as thymine. Detailed methylation status of test promoter region was determined by next generation amplicon sequencing. First PCR was carried out as mentioned above with 1 to 3µl bisulfite-converted DNA. PCR products were re-amplified by tag-specific multiplex identifier (MID) or index primer sets and the following PCR conditions: 95 °C for 15 min, (95 °C for 30 s, annealing temperature for 30 s, 72 °C for 45 s) 45 cycles (Flp-In T-REx 293) or 55 (Flp-In T-REx HeLa) cycles, 72 °C for 10 min. Processing of samples on the Roche 454 Junior (Flp-In T-REx 293) or MiSeq (Flp-In T-REx HeLa) platform and analysis using the Amplikyzer program was performed as described (Rahmann et al., 2013; Leitao et al., 2018). The program checks efficiency of bisulfite conversion by determining the C/T conversion rate at non-CpG cytosines. Only reads with a conversion rate >95% were included in the analysis. The output is represented as heatmaps, with reads in rows, single CpG sites in columns. Methylated CpGs are shown in red, non-methylated CpGs in blue (Figure 1B). Primers are listed in Table S1.

2.7. Lentiviral transduction

For lentivirus production, HEK293FT cells were seeded at 5×10^5 cells/10cm dish in DMEM complete (DMEM, 10% FBS, 1% penicillin/streptomycin (all Thermo Fisher Scientific, #41966, #10270, #15140122)). 4 hours before transfection medium was changed into medium without antibiotics. Transfection was performed 24 h after seeding, using Fugene HD (Promega, #E2311), lentiviral packaging plasmids (1.5 µg VSV-G/pMD2, 3 µg pSPAX, Table S2; provided by Alexander Schramm, University Hospital Essen) and 3µg of plasmid pLJM1-DNMT3A2 (Table S2; provided by Wolfgang Wagner, University Hospital Aachen, Bozic et al., 2018). 24 hours after transfection, DMEM complete medium was changed. 72 hours after transfection supernatant containing virus particles was harvested, filtered (0.45µm PES membrane filter; VWR, #514-0075) and stored at -80 °C. For transduction, Flp-In T-REx HeLa were seeded at 6×10^4 cells/well in a 6-well plate and treated with 500µl virus supernatant 24 h after seeding. Selection of stable Flp-In T-REx HeLa DNMT3A2 cells was started 48 h after transduction by maintaining cells in culture medium with 0.2 µg/ml puromycin (Sigma, #P8833).

2.8. Transient transfections

For transient transfection, Flp-In T-REx HeLa were seeded at 2×10^5 cells/well in a 6-well plate in tetracycline-free medium and transfected using Fugene HD (Promega, #E2311), 500 ng of pLJM1-DNMT3A2 plus 500ng pCMV6-XL5-DNMT3L plasmids (Table S2). 48 hours after transient transfection, CMV promoter activity was induced for three days by doxycycline (Sigma, #D9891, final concentration 1 µg/ml) with daily medium change.

2.9. Analyses and statistics

Analyses and graphical display of qPCR results were performed in GraphPad Prism 8 (GraphPad Software). Unless otherwise stated, Mann-Whitney test was used for testing statistical significance. Significance levels: ns: not significant, *$p \leq 0.05$, **$p \leq 0.01$, ***$p \leq 0.001$, ****$p \leq 0.0001$.

3. Results

The human model for investigating the effect of transcriptional read-through on gene repression and acquisition of DNA methylation was established in the Flp-In T-REx cell system, which carries stable integrations of an expression cassette for the tetracycline repressor and a single FRT site (Figure 2A). A targeting vector is used to integrate a gene of interest under control of the doxycycline inducible CMV promoter by recombination via the FRT site. Here, the targeting vector does not contain a cDNA of interest, but a fragment of the rabbit β-globin gene (*ocHBB2*; exon 2–intron 2–exon 3, Latos et al., 2012; Sleutels et al., 2002) (Figure 2B). Test promoters driving expression of reporter transcripts (*EGFP* or *exon1/3*, see below) were integrated into intron 2 of *ocHBB2*. Expression of the transcript *ocHBB2* exon 2/exon 3 (designated *ocHBB2* throughout the text) is driven by the CMV promoter upon induction with doxycycline. The benefit of this system is that all integrations occur at the same site in the genome, avoiding position effects associated with random integrations. In addition, embedding the targeting construct into the genome ensures packaging into the nucleosome environment of the integration site and enables regulation by histone modifications and DNA methylation.

3.1. Investigation of transcriptional interference

For studying transcriptional interference, a minigene consisting of test promoter and *EGFP* was inserted into intron 2 of *ocHBB2* either in sense or in antisense direction (Figure 3A). In sense orientation, inserted transcripts used the poly-adenylation (pA) signal of the *ocHBB2* gene fragment. For antisense constructs, we introduced a pA signal at the 3′ end of *EGFP*. Promoter fragments used were *UBE3A*, *MSH2*, *HBA2* and *SNRPN* (Figure S2). The *HBA2* promoter was amplified as *HBA2*-short, which contains the region directly upstream of the *HBA2* transcriptional start site, and *HBA2*-long, which contains the full CpG island. All promoter fragments contained single nucleotide variants to enable discrimination between introduced and endogenous promoters in DNA methylation analyses. Promoter activity of the amplified and cloned promoter fragments was confirmed by luciferase reporter assays (Figure S3A). Addition of doxycycline had no influence on the activity of promoter fragments (Figure S3B).

Four stable cell lines on the Flp-In T-REx 293 background were generated. Corresponding to the endogenous loci, the minigenes (promoter plus *EGFP*) were inserted in antisense (*UBE3A*, *HBA2*) and sense (*MSH2, SNRPN*) orientation relative to the CMV promoter, designated $UBE3A^{AS}$, $HBA2^{AS}$_short, $HBA2^{AS}$_long, $MSH2^{S}$ and $SNRPN^{S}$_GFP. Data for $HBA2^{AS}$_long are shown in Figure S4 and for $SNRPN^{S}$_GFP in Figure S5. For each cell line, three independently generated clones were used for experiments. First, the influence of CMV promoter induction on expression of the reporter gene *EGFP* was assessed. CMV promoter activity was induced for three and 14 days, and induction of *ocHBB2* was observed in all cell lines. The level of induction was comparable in all cell lines. But in $MSH2^{S}$, cell clone dependent variability was observed (Figure 3B). Without induction of the CMV promoter, *EGFP* expression was detected on RNA level in all cell lines and at the protein level in lines $UBE3A^{AS}$, $HBA2^{AS}$_short, $HBA2^{AS}$_long, but not in $MSH2^{S}$ and $SNRPN^{S}$_GFP (Figure 3B, S4, S5, S6). Upon induction of the CMV promoter by doxycycline, *EGFP* expression decreased in all cell lines, with strongest effect observed in $UBE3A^{AS}$ on RNA and protein level (Figure 3B, S6), which suggests induction of transcriptional interference. Again, $MSH2^{S}$ showed highest variability, which was cell clone dependent. *ocHBB2* induction and *EGFP* repression levels did not change during the 14-day time course of the experiment, suggesting rapid establishment of a steady-state level after doxycycline induction. In patient tissue, *HBA2* and *MSH2* promoters become silenced permanently by DNA methylation following transcriptional interference. In our model, none of the $UBE3A^{AS}$, $HBA2^{AS}$_short, $HBA2^{AS}$_long and $MSH2^{S}$ promoters became methylated after three and 14 days of induction as shown by next

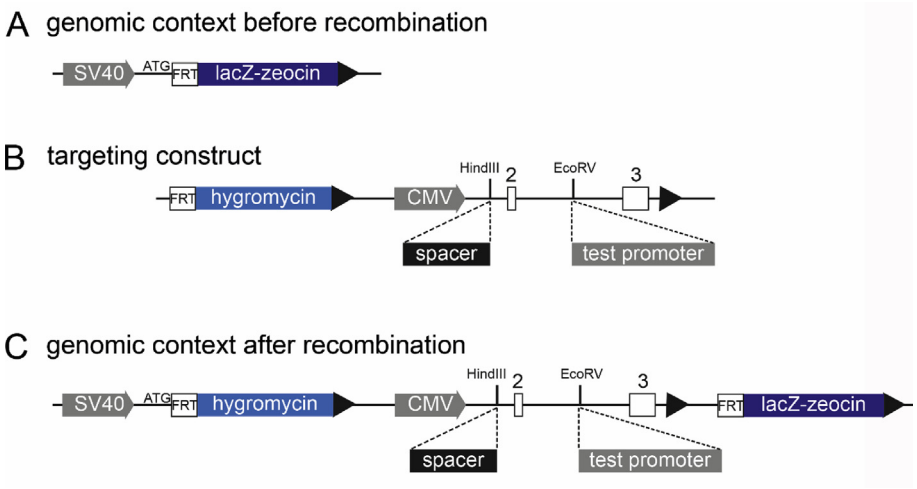

Figure 2. Site-specific integration into the genome of Flp-In T-REx cells. A) In Flp-In T-REx host cells a *Flp recombinase* target site (FRT) and the fusion selection gene LacZ-zeocin (blue) under the SV40 promoter was randomly integrated in single copy into the genome. B) Targeting construct. Backbone of pcDNA5/FRT/TO carries an FRT site, the hygromycin resistance gene and the inducible CMV promoter (CMV). The *ocHBB2* exon 2 - intron 2 - exon 3 array was integrated downstream of the CMV promoter. The HindIII site was used to integrate spacer sequence, EcoRV was used to integrate test promoters. C) After Flp-mediated recombination, the ATG is now used for translation of the hygromycin resistance gene. Inducible and test promoters are integrated at a unique genomic position. Presence of spacer depends on construct. Specific constructs are depicted at corresponding Figures.

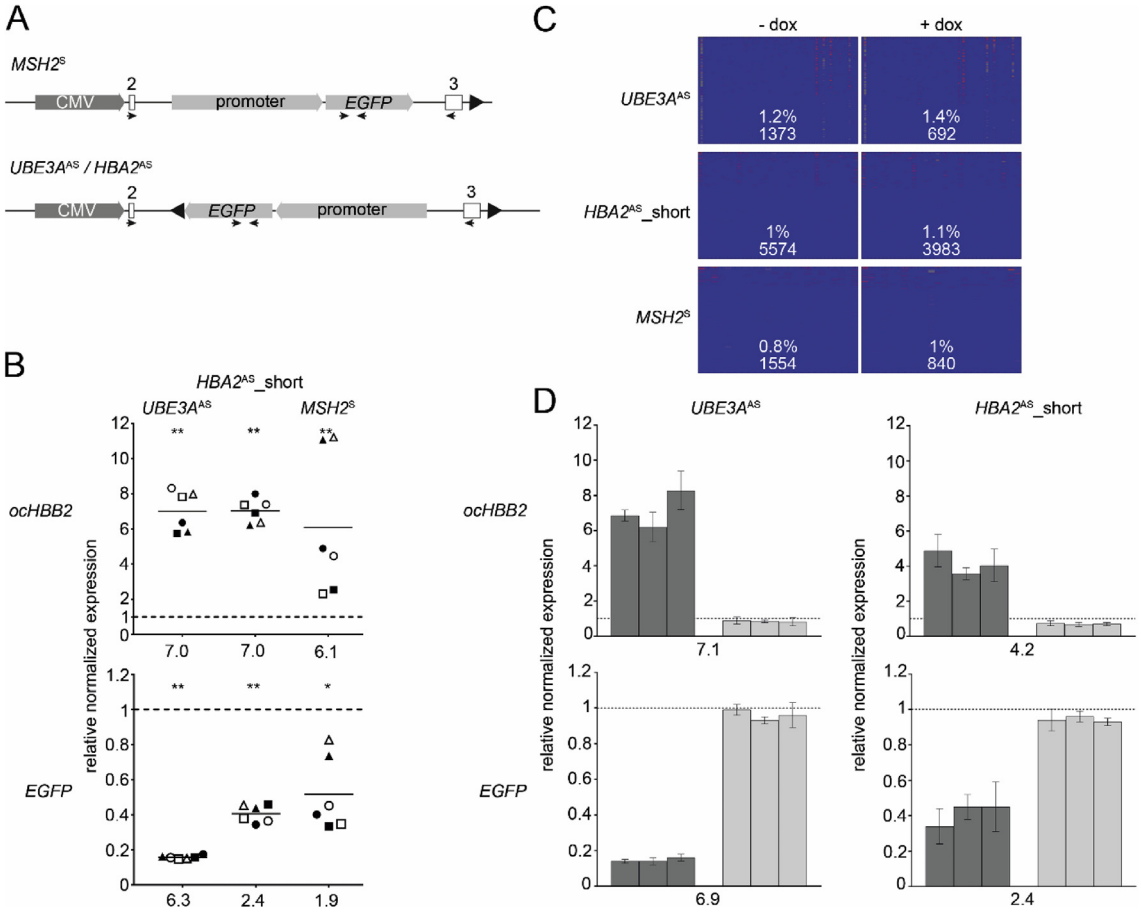

Figure 3. Expression and methylation analyses in Flp-In T-REx 293. A) Targeting constructs. Dark grey: upstream CMV promoter, light grey: minigene consisting of test promoter *(MSH2, HBA2, UBE3A)* and *EGFP*, white: exons 2 and 3 of *ocHBB2*, triangle: poly(A) signal, black bar: linker for integration of minigenes, arrows: primers for qRT-PCR. B) Expression of *ocHBB2* (top) and *EGFP* (bottom) upon induction with doxycycline, black: 3 days, white 14 days. Short line indicates mean fold induction/reduction, number below indicates fold change relative to uninduced state, dotted line: uninduced set to 1. Symbols: independent clones. C) DNA methylation of test promoters before and after induction (-/+ dox). Blue: not methylated, red: methylated, CGs in columns, reads in rows. Overall percentage of DNA methylation and number of reads are indicated. In comparison to the example plot in Figure 1B, there are no methylated (red) reads. D) Expression of *ocHBB2* (top) and *EGFP* (bottom) after 3 days induction (dark grey bars) and after 3 days without induction (light grey bars). Numbers below indicate average fold change between these two states. Dotted line: uninduced state set to 1.

generation bisulfite sequencing analysis (Figure 3C, S4C). *SNRPN*^{S}_GFP also did not acquire DNA methylation as analyzed by Sanger sequencing after bisulfite conversion (data not shown). Therefore, reversibility of *EGFP* repression was examined. Cell lines *UBE3A*^{AS}, *HBA2*^{AS}_short, *HBA2*^{AS}_long and *SNRPN*^{S}_GFP were induced with doxycycline for three days and analyzed after another three days without induction (Figure 3D, S4D S5C). *MSH2*^{S} cell lines were not included because of the high variability in effects (Figure 3B). Three days of *ocHBB2* induction resulted in

decreased expression of *EGFP*, which was reversed during the following three days without induction (Figure 3D, S4D, S5C). This demonstrated that repression of *EGFP* is directly dependent on transcription of *ocHBB2*.

3.2. Attempts to induce DNA methylation by transcriptional read-through

For further studying transcriptional interference at tandem promoters and the establishment of DNA methylation by transcriptional read-through, we used Flp-In T-REx HeLa cells, as these expressed *DNMT3A* at a higher level than Flp-In T-REx 293 cells (Figure S7). The targeting vector was modified to include a 1kb spacer element, which enhances the distance between the upstream inducible CMV promoter and the integrated downstream promoter. In addition, the *EGFP* reporter gene was omitted (Figure 4A). The promoter sequences, including endogenous exon 1 of *MSH2* and *SNRPN* were inserted into intron 2 of the *ocHBB2* gene fragment in tandem orientation to the upstream CMV promoter. The CMV promoter again drove transcription of *ocHBB2*, whereas the *MSH2* and *SNRPN* promoters drove expression of a transcript consisting of the respective endogenous exon 1 and exon 3 of *ocHBB2* (designated exon 1/3 transcript) (Figure 4A). Single nucleotide variants were introduced into both promoter fragments to enable discrimination from the endogenous promoter sequences in methylation analyses. The *MSH2* promoter fragment was additionally modified at four cryptic splice sites to suppress aberrant splicing of *ocHBB2* exon 2 on *MSH2* exon 1 (Figure S2), which had been observed in preliminary experiments (not shown). Activity of promoter fragments was tested in luciferase assays and doxycycline had no influence on promoter activity (Figure S3).

The promoter constructs were used to establish two stable Flp-In T-REx HeLa cell lines, designated *MSH2*^{S}_ex1 and *SNRPN*^{S}_ex1. Per cell line, expression was analyzed in three independently generated clones at three and 14 days of induction by doxycycline. In *SNRPN*^{S}_ex1, transcription of *ocHBB2* was induced about 2-fold, whereas *MSH2*^{S}_ex1 reached a mean induction level of almost 24-fold (Figure 4B). Induction was comparable at both time points and among independent clones. Transcription of exon 1/3 transcript driven by *SNRPN* and *MSH2* promoter fragments was decreased upon three and 14 days of induction, compared to the not induced state (Figure 4B). Induction of *ocHBB2* correlated with suppression of *MSH2* and *SNRPN* promoter activity, indicating silencing by transcriptional read-through. However, silencing was not followed by DNA methylation in any of the cell lines, as analyzed by bisulfite-based Sanger sequencing (data not shown). Decreased expression of *MSH2 and SNRPN* exon1/3 transcripts after three days of *ocHBB2* induction was reversed during the following three days without induction (Figure 4C). Repression of *MSH2 and SNRPN* exon1/3 was therefore directly dependent on *ocHBB2* transcriptional read-through.

Probably, the level of DNMT3A2 in Flp-In T-REx HeLa cells was not sufficient for induction of de novo DNA methylation. To increase the levels of DNMT3A2, a *DNMT3A2* expression cassette was stably integrated in Flp-In T-REx HeLa cells by lentiviral transduction, followed by integration of the *MSH2* and *SNRPN* promoter constructs. In these cell lines (*MSH2*^{S}_ex1_DNMT3A2 and *SNRPN*^{S}_ex1_DNMT3A2), increased *DNMT3A2* expression was detected at RNA but not protein level (Figure S8A, B). In these modified cell lines, induction of *ocHBB2,* repression of exon 1/3 and failure of DNA methylation acquisition were comparable to experiments in non-transduced Flp-In T-REx HeLa cells (Figures S8C, D). To obtain very high levels of DNTM3A2 and DNMT3L, these proteins were transiently overexpressed (Figure S9). Following transfection of the *MSH2*^{S}_ex1_DNMT3A2 and *SNRPN*^{S}_ex1_DNMT3A2 cell lines with *DNMT3A2* and *DNMT3L* expression plasmids, RNA and protein expression levels of the two proteins increased substantially

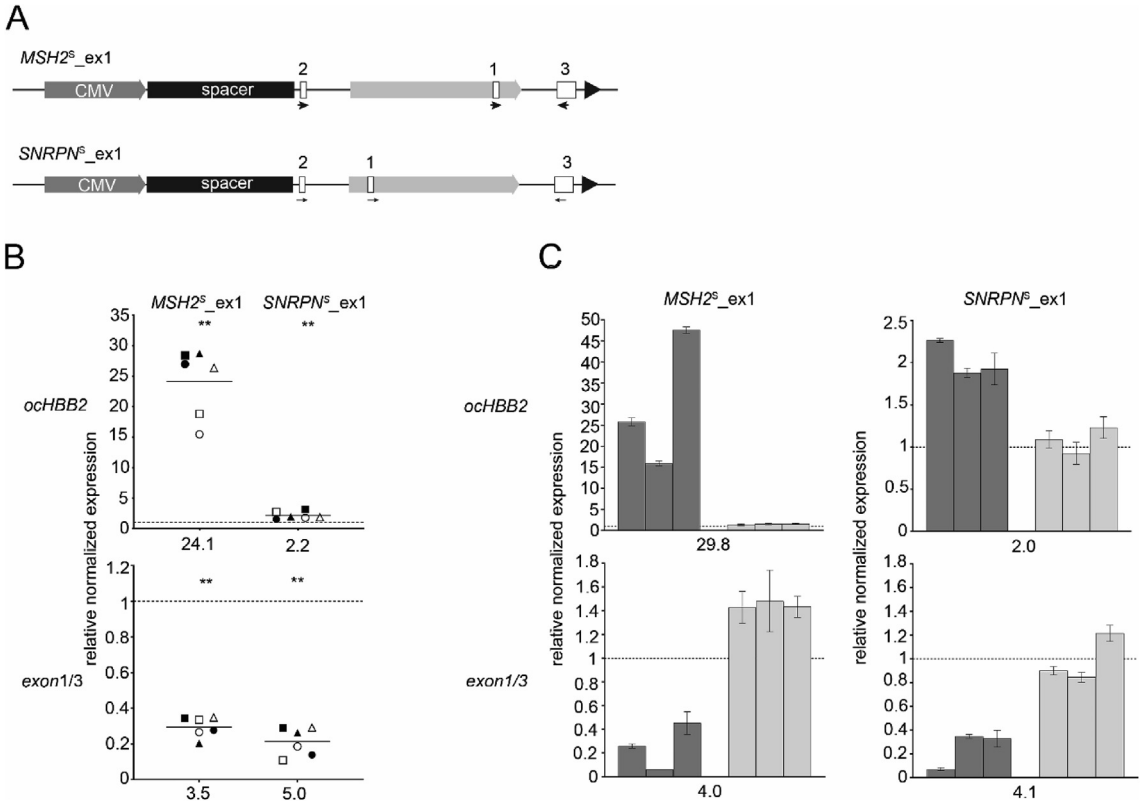

Figure 4. Expression analyses in Flp-In T-Rex HeLa. A) Targeting constructs. Dark grey: upstream CMV promoter, black: spacer sequence, light grey: test promoter *(MSH2, SNRPN)*, white: exons of *ocHBB2* and endogenous exon 1, triangle: poly(A) signal, arrows: primers for qRT-PCR. B) Expression of *ocHBB2* (top) and exon1/3 (bottom) upon induction with doxycycline: black: 3 days, white: 14 days. Short line indicates mean fold induction/reduction and numbers below indicate fold change relative to uninduced state (set to 1, dotted line). Symbols: independent clones. C) Expression of *ocHBB2* (top) and *EGFP* (bottom) after 3 days induction (dark grey bars) and again after 3 days without induction (light grey bars). Numbers below indicate average fold change between these two states. Dotted line: uninduced state set to 1.

(Figure S9, S10). Trends in expression changes of *ocHBB2* and repression of exon 1/3 transcripts were comparable to the previous experiments (Figure 5A). But again, analysis of DNA methylation by next-generation bisulfite sequencing showed no acquisition of DNA methylation in any cell line (Figure 5B).

4. Discussion

We have developed a simple and versatile human cell culture system to study the role of transcription in gene silencing and de novo DNA methylation. Induction of upstream transcription of *ocHBB2* initiating at the CMV promoter consistently resulted in repression of the downstream inserted promoters. *MSH2* and *SNRPN* promoters were weak promoters inserted in tandem orientation, whereas *UBE3A* and *HBA2* were relatively strong promoters orientated antisense to the CMV promoter. Induction of *ocHBB2* reduced expression of the *EGFP* reporter gene in Flp-In T-REx 293 cells and of exon1/3 in Flp-In T-REx HeLa cells. Repression was dependent on *ocHBB2* transcription. We showed that the system is capable of modelling transcriptional interference, independently of cell line, orientation and strength of promoters. However, DNA methylation did not follow transcriptional repression in any of the generated cell lines.

Acquisition of DNA methylation as consequence of transcriptional read-through has been demonstrated at several genomic loci. In natural genomic context, transcriptional read-through is needed for establishment of gametic imprints (see introduction). The role of transcriptional read-through for establishment of DNA methylation was strengthened further by the observation of rare patients with α-thalassemia, Lynch syndrome and methylmalonic acidemia with homocystinuria type cblC (Gueant et al., 2018; Ligtenberg et al., 2009; Tufarelli et al., 2003). These cases showed that somatic cells contain all factors necessary for the induction of DNA methylation. It consequently should be possible to mimic this mechanism in the somatic cell culture system described here.

De novo DNA methylation is mediated by the two DNA methyltransferases DNMT3A and DNMT3B. Knock-out of *Dnmt3A* and/or *Dnmt3B* is lethal in mice (Okano et al., 1999). In humans, somatic mutations in *DNMT3A* and *DNMT3B* have been described in AML, Tatton-Brown-Rahmann syndrome and ICF syndrome (Tatton-Brown et al., 2014; Xu et al., 1999; Yan et al., 2011). DNMT3A and DNMT3B are very similar in structure and biochemically, their catalytic activity is enhanced on interaction with DNMT3L, which itself has no methyltransferase activity (Suetake et al., 2004). Both DNMTs were shown to bind to H3K36me in vitro (DNMT3A) or in vivo (DNMT3B) (Baubec et al., 2015; Dhayalan et al., 2010). Despite these similarities in structure and binding partners, in vivo studies showed that DNMT3A and DNMT3B have different functions and target specificities, depending on the cellular context. DNMT3A and DNMT3L are essential for establishment of DNA methylation in germ cells. In oocytes, establishment of maternal imprints and in sperm silencing of retrotransposons as well as establishment of paternal imprints are dependent on presence of these two factors (Bourc'his and Bestor, 2004; Bourc'his et al., 2001; Kaneda et al., 2004; Suetake et al., 2004). The function of DNMT3A in oocytes is dependent on presence of its cofactor DNMT3L and of SETD2, the histone methyltransferase catalyzing tri-methylation of H3K36 (Bourc'his et al., 2001; Xu et al., 2019). In somatic cells, DNMT3A exhibited a preference for H3K36me2 rather than for H3K36me3 and acts independently of DNMT3L (Weinberg et al., 2019). However, Duymich et al. showed that catalytically inactive isoforms of DNMT3B could act as cofactors for DNMT3A, possibly replacing DNMT3L in somatic cells (Duymich et al., 2016). H3K36me2 is established by NSD1 and enriched in intergenic regions. Ablation of NSD1 in mouse cells resulted in loss of H3K36me2, subsequent failure of recruitment of DNMT3A and hypomethylation of intergenic regions (Weinberg et al., 2019). Specific patterns of DNA hypomethylation were also identified in the human overgrowth syndromes Sotos syndrome and Tatton-Brown-Rahmann syndrome, which are similar in phenotype and are caused by mutations in NSD1 and DNMT3A, respectively (Choufani et al., 2015; Tatton-Brown et al., 2014; Weinberg et al., 2019). In contrast to Dnmt3A, Dnmt3B is essential for de novo DNA methylation during early embryogenesis, but not in germ cells (Kaneda et al., 2004; Okano et al., 1999). In mouse ES cells, specifically DNMT3B was recruited to sites of active transcription, which are marked by H3K36me3, mediated by SETD2 (Baubec et al., 2015). In our cell system, DNMT3A, DNMT3B, SETD2 and NSD1 were expressed, while DNMT3L was absent, as expected for differentiated cells (Figure S7C, Lucifero et al., 2007; Okano et al., 1998). However, simply elevating the expression level of DNMT3A2 and DNMT3L in the Flp-In T-REx HeLa system still did not result in establishment of DNA methylation at the tested promoters (Figure 5B, S8D).

The question is, if DNA methylation is not established or if it is not maintained. For maintenance of DNA methylation at imprinted genes, DNMT1 and ZFP57 are known to be essential. DNMT1 is expressed in our cell system, whereas ZFP57 is not (Figure S7C). ZFP57 is a KRAB-domain

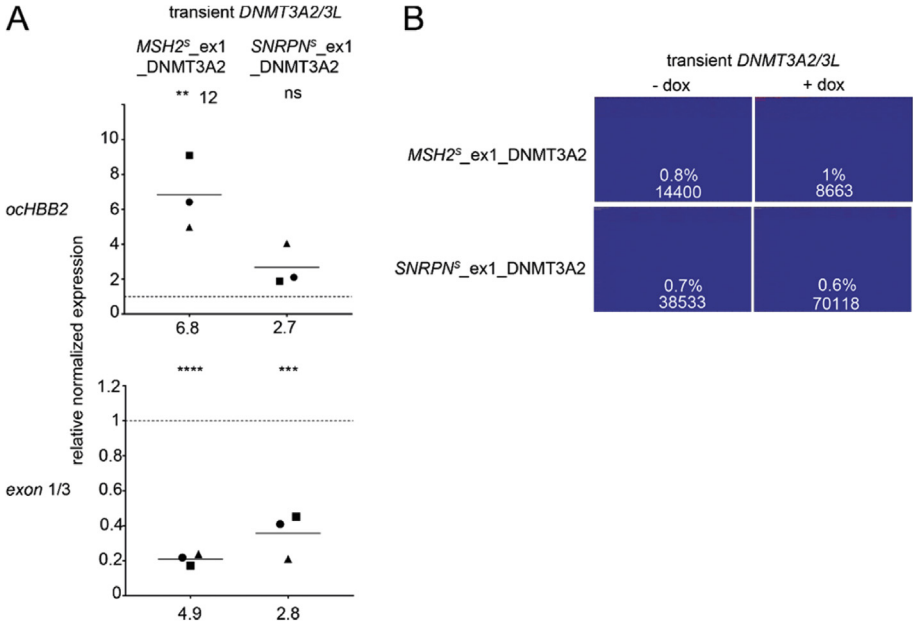

Figure 5. Transient overexpression of DNMT3L and DNMT3A2. A) Expression of *ocHBB2* (top) and exon1/3 (bottom) upon induction with doxycycline in *MSH2*^{S}-ex1_DNMT3A2 and *SNRPN*^{S}_ex1_DNMT3A2 for three days. Short line indicates mean fold induction/reduction, numbers below indicate fold change relative to uninduced state (set to 1, dotted line). Symbols: independent clones. Statistical analysis with Student t-test. B) DNA methylation of test promoters before and after induction (-/+ dox). Blue: not methylated, red: methylated, CGs in columns, reads in rows. Overall percentage of DNA methylation and number of reads are indicated. In comparison to the example plot in Figure 1B, there are no methylated (red) reads.

containing zinc finger protein, which binds to methylated DNA in a sequence specific manner and recruits DNA methyltransferases DNMT1, DNMT3A and DNMT3L via the mediator protein KAP1 (Quenneville et al., 2011; Zuo et al., 2012). In mice, oocyte and zygotic Zfp57 is essential for maintenance of DNA methylation at imprinted regions during development (Li et al., 2008; Strogantsev et al., 2015). In humans, ZFP57 is not expressed in oocytes, but expression in early embryonic development is needed for methylation maintenance at specific imprinted differentially methylated regions, like *PLAGL1*:alt-TSS-DMR, *PEG3*:TSS-DMR and *GRB10*:alt-TSS-DMR (Mackay et al., 2008; Okae et al., 2014).

Since provision of DNMT3A2 and DNMT3L at high levels did not result in DNA methylation as consequence of transcriptional read-through at the analyzed promoters, we speculate that the genomic context could be a problem in the cell systems. The Flp-In T-REx cell system allows integration of constructs as a single copy using an FRT-site at a fixed, but unknown, genomic position. Therefore, we can exclude position effects caused by different genomic integration sites. Unlike many other transgenes, our constructs were not methylated by a host-defense mechanism, but also not by induction of transcriptional read-through. However, the cell culture system described here does not reflect the normal genomic environment at the individual loci. At the *SNURF-SNRPN* locus, the distance between the upstream AS-SRO and PWS-SRO is 35kb. In Lynch syndrome patients the distance between *EPCAM* and *MSH2* promoter is about 16kb. The distance between the inducible upstream CMV promoter and the investigated test promoter in our cell system ranges from 211 to 1282 base pairs, which is far less than observed in natural context. This could result in steric hindrance of protein complexes that need access for transcription, modifying histones and establishing DNA methylation.

Another explanation for failure to induce DNA methylation may relate to the strength of the CMV and test promoters and the kinetics of transcription of the constructs. It is possible that de novo methylation occurs only within a narrow window of the relative strength of the upstream and downstream promoters, which is met at the endogenous imprinted and disease loci, but not in our constructs.

In summary, we have established a cell culture system to examine transcriptional interference and transcriptional read-through of human promoters in somatic cells. The strength of our system is that there are no position effects and that transcription from one promoter is inducible by doxycycline. We show that transcriptional interference leads to transient repression of the sensitive promoter, but that transcriptional read-through is not sufficient for inducing DNA methylation. We note that transcriptional read-through is also not sufficient to induce an epigenetic switch in the silencing activity of Polycomb response elements (Erokhin et al., 2015). Establishment of DNA methylation is a complex process, which requires the presence of specific factors at the right amount and the right time. Probably, it also depends on the genomic context of the target region including adjacent regulatory elements as well as the strength of the transcription processes. We recommend conducting further investigations into the role of the genomic context, for example by replacing regular promoters by an inducible promoter. With the advent of CRISPR/Cas9 genome engineering such experiments could be done, if the integrated promoter is not silenced by the host-defense system.

Declarations

Author contribution statement

T. Kühnel: Conceived and designed the experiments; Performed the experiments; Analyzed and interpreted the data; Wrote the paper.

H. Heinz: Conceived and designed the experiments; Performed the experiments; Analyzed and interpreted the data.

N. Utz: Performed the experiments; Analyzed and interpreted the data.

T. Boszic: Contributed reagents, materials, analysis tools or data.

B. Horsthemke and L. Steenpass: Conceived and designed the experiments; Analyzed and interpreted the data; Wrote the paper.

Funding statement

This work was supported by the Deutsche Forschungsgemeinschaft (Grants HO949/22-1, STE1987/3-1, STE1987/5-1 and Research Training Group 1431 Transcription, Chromatin Structure and DNA Repair in Development and Differentiation).

Competing interest statement

The authors declare no conflict of interest.

Additional information

Supplementary content related to this article has been published online at https://doi.org/10.1016/j.heliyon.2020.e03261.

Acknowledgements

We thank Claudia Mertel and Michaela Hiber for excellent technical assistance, Dr. Sophie Kalmbach for performing lentiviral transduction and Prof. Hemmo Meyer, University Duisburg-Essen, for providing Flp-In T-REx HeLa cells. We also acknowledge Dr. Jasmin Beygo for performing the PWS-SRO methylation analysis shown in Figure 1B.

References

Baubec, T., Colombo, D.F., Wirbelauer, C., Schmidt, J., Burger, L., Krebs, A.R., Akalin, A., Schubeler, D., 2015. Genomic profiling of DNA methyltransferases reveals a role for DNMT3B in genic methylation. Nature 520, 243–247.

Berretta, J., Morillon, A., 2009. Pervasive transcription constitutes a new level of eukaryotic genome regulation. EMBO Rep. 10, 973–982.

Beygo, J., Burger, J., Strom, T.M., Kaya, S., Buiting, K., 2019. Disruption of KCNQ1 prevents methylation of the ICR2 and supports the hypothesis that its transcription is necessary for imprint establishment. Eur. J. Hum. Genet. 27, 903–908.

Bordoy, A.E., Varanasi, U.S., Courtney, C.M., Chatterjee, A., 2016. Transcriptional interference in convergent promoters as a means for tunable gene expression. ACS Synth. Biol. 5, 1331–1341.

Bourc'his, D., Bestor, T.H., 2004. Meiotic catastrophe and retrotransposon reactivation in male germ cells lacking Dnmt3L. Nature 431, 96–99.

Bourc'his, D., Xu, G.L., Lin, C.S., Bollman, B., Bestor, T.H., 2001. Dnmt3L and the establishment of maternal genomic imprints. Science 294, 2536–2539.

Bozic, T., Frobel, J., Raic, A., Ticconi, F., Kuo, C.C., Heilmann-Heimbach, S., Goecke, T.W., Zenke, M., Jost, E., Costa, I.G., Wagner, W., 2018. Variants of DNMT3A cause transcript-specific DNA methylation patterns and affect hematopoiesis. Life Sci Alliance 1, e201800153.

Buiting, K., Lich, C., Cottrell, S., Barnicoat, A., Horsthemke, B., 1999. A 5-kb imprinting center deletion in a family with Angelman syndrome reduces the shortest region of deletion overlap to 880 bp. Hum. Genet. 105, 665–666.

Capuano, F., Mülleder, M., Kok, R., Blom, H.J., Ralser, M., 2014. Cytosine DNA methylation is found in Drosophila melanogaster but absent in Saccharomyces cerevisiae, Schizosaccharomyces pombe, and other yeast species. Anal. Chem. 86, 3697–3702.

Chotalia, M., Smallwood, S.A., Ruf, N., Dawson, C., Lucifero, D., Frontera, M., James, K., Dean, W., Kelsey, G., 2009. Transcription is required for establishment of germline methylation marks at imprinted genes. Genes Dev. 23, 105–117.

Choufani, S., Cytrynbaum, C., Chung, B.H., Turinsky, A.L., Grafodatskaya, D., Chen, Y.A., Cohen, A.S., Dupuis, L., Butcher, D.T., Siu, M.T., Luk, H.M., Lo, I.F., Lam, S.T., Caluseriu, O., Stavropoulos, D.J., Reardon, W., Mendoza-Londono, R., Brudno, M., Gibson, W.T., Chitayat, D., Weksberg, R., 2015. NSD1 mutations generate a genome-wide DNA methylation signature. Nat. Commun. 6, 10207.

Dhayalan, A., Rajavelu, A., Rathert, P., Tamas, R., Jurkowska, R.Z., Ragozin, S., Jeltsch, A., 2010. The Dnmt3a PWWP domain reads histone 3 lysine 36 trimethylation and guides DNA methylation. J. Biol. Chem. 285, 26114–26120.

Duymich, C.E., Charlet, J., Yang, X., Jones, P.A., Liang, G., 2016. DNMT3B isoforms without catalytic activity stimulate gene body methylation as accessory proteins in somatic cells. Nat. Commun. 7, 11453.

Erokhin, M., Elizar'ev, P., Parshikov, A., Schedl, P., Georgiev, P., Chetverina, D., 2015. Transcriptional read-through is not sufficient to induce an epigenetic switch in the silencing activity of Polycomb response elements. Proc. Natl. Acad. Sci. U.S.A. 112, 14930–14935.

Gueant, J.L., Chery, C., Oussalah, A., Nadaf, J., Coelho, D., Josse, T., Flayac, J., Robert, A., Koscinski, I., Gastin, I., Filhine-Tresarrieu, P., Pupavac, M., Brebner, A., Watkins, D., Pastinen, T., Montpetit, A., Hariri, F., Tregouët, D., Raby, B.A., Chung, W.K.,

Morange, P.E., Froese, D.S., Baumgartner, M.R., Benoist, J.F., Ficicioglu, C., Marchand, V., Motorin, Y., Bonnemains, C., Feillet, F., Majewski, J., Rosenblatt, D.S., 2018. APRDX1 mutant allele causes a MMACHC secondary epimutation in cblC patients. Nat. Commun. 9, 67.

Hobson, D.J., Wei, W., Steinmetz, L.M., Svejstrup, J.Q., 2012. RNA polymerase II collision interrupts convergent transcription. Mol. Cell. 48, 365–374.

Horsthemke, B., 2014. In Brief: genomic imprinting and imprinting diseases. J. Pathol. 232, 485–487.

Hsiao, J.S., Germain, N.D., Wilderman, A., Stoddard, C., Wojenski, L.A., Villafano, G.J., Core, L., Cotney, J., Chamberlain, S.J., 2019. A bipartite boundary element restricts UBE3A imprinting to mature neurons. Proc. Natl. Acad. Sci. U. S. A. 116, 2181–2186.

Jeziorska, D.M., Murray, R.J.S., De Gobbi, M., Gaentzsch, R., Garrick, D., Ayyub, H., Chen, T., Li, E., Telenius, J., Lynch, M., Graham, B., Smith, A.J.H., Lund, J.N., Hughes, J.R., Higgs, D.R., Tufarelli, C., 2017. DNA methylation of intragenic CpG islands depends on their transcriptional activity during differentiation and disease. Proc. Natl. Acad. Sci. U.S.A. 114, E7526–E7535.

Joh, K., Matsuhisa, F., Kitajima, S., Nishioka, K., Higashimoto, K., Yatsuki, H., Kono, T., Koseki, H., Soejima, H., 2018. Growing oocyte-specific transcription-dependent de novo DNA methylation at the imprinted Zrsr1-DMR. Epigenet. Chromatin 11, 28.

Kanber, D., Berulava, T., Ammerpohl, O., Mitter, D., Richter, J., Siebert, R., Horsthemke, B., Lohmann, D., Buiting, K., 2009. The human retinoblastoma gene is imprinted. PLoS Genet. 5, e1000790.

Kaneda, M., Okano, M., Hata, K., Sado, T., Tsujimoto, N., Li, E., Sasaki, H., 2004. Essential role for de novo DNA methyltransferase Dnmt3a in paternal and maternal imprinting. Nature 429, 900–903.

Kelsey, G., Feil, R., 2013. New insights into establishment and maintenance of DNA methylation imprints in mammals. Philos. Trans. R. Soc. Lond. B Biol. Sci. 368, 20110336.

Landers, M., Bancescu, D.L., Le Meur, E., Rougeulle, C., Glatt-Deeley, H., Brannan, C., Muscatelli, F., Lalande, M., 2004. Regulation of the large (approximately 1000 kb) imprinted murine Ube3a antisense transcript by alternative exons upstream of Snurf/Snrpn. Nucleic Acids Res. 32, 3480–3492.

Latos, P.A., Stricker, S.H., Steenpass, L., Pauler, F.M., Huang, R., Senergin, B.H., Regha, K., Koerner, M.V., Warczok, K.E., Unger, C., Barlow, D.P., 2009. An in vitro ES cell imprinting model shows that imprinted expression of the Igf2r gene arises from an allele-specific expression bias. Development 136, 437–448.

Latos, P.A., Pauler, F.M., Koerner, M.V., Senergin, H.B., Hudson, Q.J., Stocsits, R.R., Allhoff, W., Stricker, S.H., Klement, R.M., Warczok, K.E., Aumayr, K., Pasierbek, P., Barlow, D.P., 2012. Airn transcriptional overlap, but not its lncRNA products, induces imprinted Igf2r silencing. Science 338, 1469–1472.

Leitao, E., Beygo, J., Zeschnigk, M., Klein-Hitpass, L., Bargull, M., Rahmann, S., Horsthemke, B., 2018. Locus-Specific DNA Methylation Analysis by Targeted Deep Bisulfite Sequencing. Methods Mol Biol 1767, 351–366. https://doi.org/10.1007/978-1-4939-7774-1_19.

Lewis, M.W., Brant, J.O., Kramer, J.M., Moss, J.I., Yang, T.P., Hansen, P.J., Williams, R.S., Resnick, J.L., 2015. Angelman syndrome imprinting center encodes a transcriptional promoter. Proc. Natl. Acad. Sci. U. S. A. 112, 6871–6875.

Lewis, M.W., Vargas-Franco, D., Morse, D.A., Resnick, J.L., 2019. A mouse model of Angelman syndrome imprinting defects. Hum. Mol. Genet. 28, 220–229.

Li, X., Ito, M., Zhou, F., Youngson, N., Zuo, X., Leder, P., Ferguson-Smith, A.C., 2008. A maternal-zygotic effect gene, Zfp57, maintains both maternal and paternal imprints. Dev. Cell 15, 547–557.

Ligtenberg, M.J., Kuiper, R.P., Chan, T.L., Goossens, M., Hebeda, K.M., Voorendt, M., Lee, T.Y., Bodmer, D., Hoenselaar, E., Hendriks-Cornelissen, S.J., Tsui, W.Y., Kong, C.K., Brunner, H.G., van Kessel, A.G., Yuen, S.T., van Krieken, J.H., Leung, S.Y., Hoogerbrugge, N., 2009. Heritable somatic methylation and inactivation of MSH2 in families with Lynch syndrome due to deletion of the 3' exons of TACSTD1. Nat. Genet. 41, 112–117.

Lucifero, D., La Salle, S., Bourc'his, D., Martel, J., Bestor, T.H., Trasler, J.M., 2007. Coordinate regulation of DNA methyltransferase expression during oogenesis. BMC Dev. Biol. 7, 36.

Mackay, D.J., Callaway, J.L., Marks, S.M., White, H.E., Acerini, C.L., Boonen, S.E., Dayanikli, P., Firth, H.V., Goodship, J.A., Haemers, A.P., Hahnemann, J.M., Kordonouri, O., Masoud, A.F., Oestergaard, E., Storr, J., Ellard, S., Hattersley, A.T., Robinson, D.O., Temple, I.K., 2008. Hypomethylation of multiple imprinted loci in individuals with transient neonatal diabetes is associated with mutations in ZFP57. Nat. Genet. 40, 949–951.

Marinus, M.G., Løbner-Olesen, A., 2009. DNA methylation. EcoSal Plus.

Meng, L., Person, R.E., Huang, W., Zhu, P.J., Costa-Mattioli, M., Beaudet, A.L., 2013. Truncation of Ube3a-ATS unsilences paternal Ube3a and ameliorates behavioral defects in the Angelman syndrome mouse model. PLoS Genet. 9, e1004039.

Numata, K., Kohama, C., Abe, K., Kiyosawa, H., 2011. Highly parallel SNP genotyping reveals high-resolution landscape of mono-allelic Ube3a expression associated with locus-wide antisense transcription. Nucleic Acids Res. 39, 2649–2657.

Okae, H., Chiba, H., Hiura, H., Hamada, H., Sato, A., Utsunomiya, T., Kikuchi, H., Yoshida, H., Tanaka, A., Suyama, M., Arima, T., 2014. Genome-wide analysis of DNA methylation dynamics during early human development. PLoS Genet. 10, e1004868.

Okano, M., Xie, S., Li, E., 1998. Cloning and characterization of a family of novel mammalian DNA (cytosine-5) methyltransferases. Nat. Genet. 19, 219–220.

Okano, M., Bell, D.W., Haber, D.A., Li, E., 1999. DNA methyltransferases Dnmt3a and Dnmt3b are essential for de novo methylation and mammalian development. Cell 99, 247–257.

Quenneville, S., Verde, G., Corsinotti, A., Kapopoulou, A., Jakobsson, J., Offner, S., Baglivo, I., Pedone, P.V., Grimaldi, G., Riccio, A., Trono, D., 2011. In embryonic stem cells, ZFP57/KAP1 recognize a methylated hexanucleotide to affect chromatin and DNA methylation of imprinting control regions. Mol. Cell. 44, 361–372.

Rahmann, S., Beygo, J., Kanber, D., Martin, M., Horsthemke, B., Buiting, K., 2013. Amplikyzer: automated methylation analysis of amplicons from bisulfite flowgram sequencing. Peer J PrePrints.

Rougeulle, C., Cardoso, C., Fontes, M., Colleaux, L., Lalande, M., 1998. An imprinted antisense RNA overlaps UBE3A and a second maternally expressed transcript. Nat. Genet. 19, 15–16.

Saeki, H., Svejstrup, J.Q., 2009. Stability, flexibility and dynamic interactions of colliding RNA polymerase II elongation complexes. Mol. Cell. 35, 191–205.

Shearwin, K.E., Callen, B.P., Egan, J.B., 2005. Transcriptional interference–a crash course. Trends Genet. 21, 339–345.

Singh, V.B., Sribenja, S., Wilson, K.E., Attwood, K.M., Hillman, J.C., Pathak, S., Higgins, M.J., 2017. Blocked transcription through KvDMR1 results in absence of methylation and gene silencing resembling Beckwith-Wiedemann syndrome. Development 144, 1820–1830.

Sleutels, F., Zwart, R., Barlow, D.P., 2002. The non-coding Air RNA is required for silencing autosomal imprinted genes. Nature 415, 810–813.

Smith, E.Y., Futtner, C.R., Chamberlain, S.J., Johnstone, K.A., Resnick, J.L., 2011. Transcription is required to establish maternal imprinting at the Prader-Willi syndrome and Angelman syndrome locus. PLoS Genet. 7, e1002422.

Strogantsev, R., Krueger, F., Yamazawa, K., Shi, H., Gould, P., Goldman-Roberts, M., McEwen, K., Sun, B., Pedersen, R., Ferguson-Smith, A.C., 2015. Allele-specific binding of ZFP57 in the epigenetic regulation of imprinted and non-imprinted monoallelic expression. Genome Biol. 16, 112.

Suetake, I., Shinozaki, F., Miyagawa, J., Takeshima, H., Tajima, S., 2004. DNMT3L stimulates the DNA methylation activity of Dnmt3a and Dnmt3b through a direct interaction. J. Biol. Chem. 279, 27816–27823.

Tatton-Brown, K., Seal, S., Ruark, E., Harmer, J., Ramsay, E., Del Vecchio Duarte, S., Zachariou, A., Hanks, S., O'Brien, E., Aksglaede, L., Baralle, D., Dabir, T., Gener, B., Goudie, D., Homfray, T., Kumar, A., Pilz, D.T., Selicorni, A., Temple, I.K., Van Maldergem, L., Yachelevich, N., Childhood Overgrowth Consortium, van Montfort, R., Rahman, N., 2014. Mutations in the DNA methyltransferase gene DNMT3A cause an overgrowth syndrome with intellectual disability. Nat. Genet. 46, 385–388.

Tufarelli, C., Stanley, J.A., Garrick, D., Sharpe, J.A., Ayyub, H., Wood, W.G., Higgs, D.R., 2003. Transcription of antisense RNA leading to gene silencing and methylation as a novel cause of human genetic disease. Nat. Genet. 34, 157–165.

Valente, F.M., Sparago, A., Freschi, A., Hill-Harfe, K., Maas, S.M., Frints, S.G.M., Alders, M., Pignata, L., Franzese, M., Angelini, C., Carli, D., Mussa, A., Gazzin, A., Gabbarini, F., Acurzio, B., Ferrero, G.B., Bliek, J., Williams, C.A., Riccio, A., Cerrato, F., 2019. Transcription alterations of KCNQ1 associated with imprinted methylation defects in the Beckwith-Wiedemann locus. Genet. Med. 21, 1808–1820.

Veselovska, L., Smallwood, S.A., Saadeh, H., Stewart, K.R., Krueger, F., Maupetit-Mehouas, S., Arnaud, P., Tomizawa, S., Andrews, S., Kelsey, G., 2015. Deep sequencing and de novo assembly of the mouse oocyte transcriptome define the contribution of transcription to the DNA methylation landscape. Genome Biol. 16, 209.

Weinberg, D.N., Papillon-Cavanagh, S., Chen, H., Yue, Y., Chen, X., Rajagopalan, K.N., Horth, C., McGuire, J.T., Xu, X., Nikbakht, H., Lemiesz, A.E., Marchione, D.M., Marunde, M.R., Meiners, M.J., Cheek, M.A., Keogh, M.C., Bareke, E., Djedid, A., Harutyunyan, A.S., Jabado, N., Garcia, B.A., Li, H., Allis, C.D., Majewski, J., Lu, C., 2019. The histone mark H3K36me2 recruits DNMT3A and shapes the intergenic DNA methylation landscape. Nature 573, 281–286.

Xu, G.L., Bestor, T.H., Bourc'his, D., Hsieh, C.L., Tommerup, N., Bugge, M., Hulten, M., Qu, X., Russo, J.J., Viegas-Pequignot, E., 1999. Chromosome instability and immunodeficiency syndrome caused by mutations in a DNA methyltransferase gene. Nature 402, 187–191.

Xu, Q., Xiang, Y., Wang, Q., Wang, L., Brind'Amour, J., Bogutz, A.B., Zhang, Y., Zhang, B., Yu, G., Xia, W., Du, Z., Huang, C., Ma, J., Zheng, H., Li, Y., Liu, C., Walker, C.L., Jonasch, E., Lefebvre, L., Wu, M., Lorincz, M.C., Li, W., Li, L., Xie, W., 2019. SETD2 regulates the maternal epigenome, genomic imprinting and embryonic development. Nat. Genet. 51, 844–856.

Yan, X.J., Xu, J., Gu, Z.H., Pan, C.M., Lu, G., Shen, Y., Shi, J.Y., Zhu, Y.M., Tang, L., Zhang, X.W., Liang, W.X., Mi, J.Q., Song, H.D., Li, K.Q., Chen, Z., Chen, S.J., 2011. Exome sequencing identifies somatic mutations of DNA methyltransferase gene DNMT3A in acute monocytic leukemia. Nat. Genet. 43, 309–315.

Zuo, X., Sheng, J., Lau, H.T., McDonald, C.M., Andrade, M., Cullen, D.E., Bell, F.T., Iacovino, M., Kyba, M., Xu, G., Li, X., 2012. Zinc finger protein ZFP57 requires its co-factor to recruit DNA methyltransferases and maintains DNA methylation imprint in embryonic stem cells via its transcriptional repression domain. J. Biol. Chem. 287, 2107–2118.